International Journal of Mechanical, Industrial and Aerospace Sciences
ISSN: 2517-9950
Vol:14, No:1, 2020

Analysis of Air-Water Two-Phase Flow in a 3x3 Rod Bundle

Pei-Syuan Ruan, Ya-Chi Yu, Shao-Wen Chen, Jin-Der Lee, Jong-Rong Wang, Chunkuan Shih

***Abstract*—**This study investigated the void fraction characteristics under low superficial gas velocity (J_g) and low superficial fluid velocity (J_f) conditions in a 3x3 rod bundle geometry. Three arrangements of conductivity probes were set to measure the void fraction at various cross-sectional regions, including rod-gap, sub-channel and rod-wall regions. The experimental tests were performed under the flow conditions of J_g = 0-0.236 m/s and J_f = 0-0.142 m/s, and the time-averaged void fractions were recorded at each flow condition. It was observed that while the superficial gas velocity increases, the small bubbles started to cluster together and become big bubbles. As the superficial fluid velocity increases, the local void fractions of the three test regions will get closer and the bubble distribution will be more uniform across the cross section.

***Keywords*—**Conductivity probes, rod bundles, two-phase flow, void fraction.

I. Introduction

TWO-PHASE flow is a flow system consisting of two different phases. Two-phase flow will carry out many different types of flow patterns because of the external conditions such as void fraction, physical properties of fluid and gas, flow channel size and geometry, temperature, and pressure drop. Two-phase flow regimes have been separated into several parts, such as bubbly flow, slug flow, churn flow and annular flow [1], [2]. Two-phase flow analysis plays an important role in safety analysis of nuclear reactors. Therefore, the two-phase flow characteristics are needed to be analyzed in more detail.

Chen et al. [3], [4] have developed the one-dimensional drift-flux model in rod bundle and compared with some existing models. However, their test condition is under pool condition and they have measured all cross section void fractions. In this study, the ranges of the test flow conditions cover $J_f \approx$ 0.024, 0.099 and 0.142 m/s, and $J_g \approx$ 0.024-0.236 m/s. The local void fraction is measured to determine the bubble distribution in detail.

Pei-Syuan Ruan is with the Department of Engineering and System Science, National Tsing Hua University, Hsinchu, 300 Taiwan (corresponding author, phone: 886-3-5715131 ext.34221; e-mail: s103011120@gmail.com).

Ya-Chi Yu is with the Department of Engineering and System Science, National Tsing Hua University, Hsinchu, 300 Taiwan.

Shao-Wen Chen and Chunkuan Shih are with the Institute of Nuclear Engineering and Science, National Tsing Hua University, Hsinchu, 300 Taiwan.

Jin-Der Lee is with the Nuclear Science & Technology Development Center, National Tsing Hua University, Hsinchu, 300 Taiwan.

Jong-Rong Wang is with the Nuclear and New Energy Education and Research Foundation, Hsinchu, 300 Taiwan.

II. Experimental Facility

Fig. 1 shows the schematic of the test facility. The purified water from the water tank is pumped into the mixer and mixes with the normal air from the compressed air tank. The flow rates of air and water can be controlled by adjusting the flow control valves such that the specific flow patterns occur. The two-phase mixture flows into the test section. The measurement region includes the three pressure sensors and several electric conductivity sensors which are around the acrylic rods and the right and left side of the casing. The test-section's horizontal cross-section is shown in Fig. 2. The experimental test conditions and the facility parameters are listed in Tables I and II. The casing of the rod bundle test section is made of 52 mm × 52 mm aluminum rectangular duct. There are a total of 9 (3 × 3) acrylic rods in the rectangular duct. The rod diameter is 11.5 mm and the rod pitch is 15.4 mm. On the top of test section is the visualization region, the rectangular duck and the rods of this region are made of transparent acrylic. The pictures of two-phase mixture in the test section will be taken by utilizing the high speed camera at the visualization region.

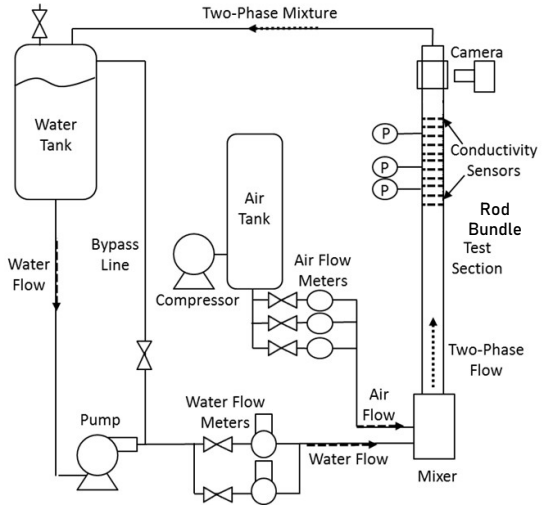

Fig. 1 Schematic of 3×3 rod bundle test facility

TABLE I
Experimental Test Conditions

Test Parameters	Test Condition
J_g(m/s)	0~0.236
J_f(m/s)	0.024, 0.099, 0.142
height of conductivity probes (cm)	270
test region	rod-gap, sub-channel and rod-wall regions

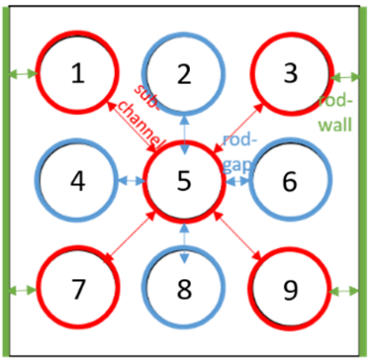

Fig. 2 Cross-sectional arrangements of conductivity probes in the rod bundle test section

TABLE II
FACILITY PARAMETERS

Facility Parameters	Values
casing size (mm)	Rectangular, 52 × 52
rod bundle	3 × 3
hydraulic diameter (mm)	9.12
rod diameter (mm)	11.5
pitch distance (mm)	15.4

During the tests, the measured voltage from conductivity probes is used to determine the void fraction of two-phase mixture. Because the difference between the dielectric constants of air and water is large, the dimensionless voltage can be used to determine the void fraction of two-phase flow mixture. The voltage of two-phase flow can be turned to dimensionless voltage by divided the voltage of full water. The relation of void fraction and dimensionless voltage is:

$$\propto = V^* = \frac{V_{two-phase}}{V_w} \quad (1)$$

where α is the void fraction, V^* is dimensionless voltage, $V_{two-phase}$ the voltage of two-phase flow, and V_w is the voltage of full water.

In the previous study [5], dimensionless voltage was applied to estimate void or liquid fraction and it has a great performance for measuring the void fraction. Chen et al. [5] used the electric conductivity sensors and 1-D drift flux model to verify the potential error of void measurement. It was found that the test data can fit the drift-flux model with limited error less than 20%.

III. Results and Discussion

A. Photography Analysis

The visualization region is on the top of test section. The pictures of two-phase flow mixtures were taken by a high speed camera of this section to observe the two-phase flow in the rod bundle. Fig. 3 shows the picture of the two-phase mixture. The superficial fluid velocity is 0.142 m/s, and the superficial gas velocities are 0.047 m/s, 0.094 m/s, 0.165 m/s and 0.236 m/s respectively. The sizes of bubbles will be larger and the number of bubbles will be greater as superficial gas velocities increases.

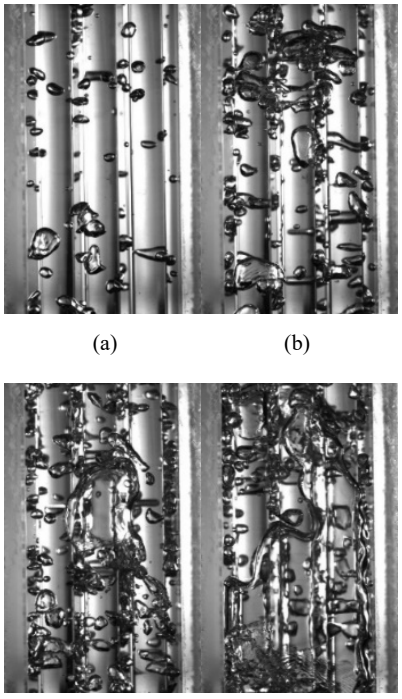

(a) (b)

(c) (d)

Fig. 3 Exemplary photos of two-phase flow in the rod bundle: (a) J_f=0.142 m/s, J_g=0.047 m/s; (b) J_f=0.142 m/s, J_g=0.094 m/s; (c) J_f=0.142 m/s, J_g=0.165 m/s; (d) J_f=0.142 m/s, J_g=0.236 m/s

B. Void Fraction Analysis

The position of the chosen electrode sensors is at 2.7 m height. Fig. 2 shows the electrode sensors which were chosen to detect the conductivity in this study. The void fraction of rod-gap, sub-channel and rod-wall regions will be discussed. The region of rod-gap is between central rod and four side rods. The sub-channel region is between central rod and four diagonal rods. Between four diagonal rods and walls is the region of rod-wall.

The signals of each condition are recorded for 120 seconds. Fig. 4 shows the signals during 55 seconds to 65 seconds of the void fraction which are transferred from the conductivity signals detected by the conductivity probes. The test conditions of Figs. 4 (a)-(d) are J_f=0.142 m/s, J_g=0.047 m/s; J_f=0.142 m/s, J_g=0.094 m/s; J_f=0.142 m/s, J_g=0.165 m/s; and J_f=0.142 m/s, J_g=0.236 m/s, respectively. In Fig. 4, there are many fluctuations of void fraction signals and there are sometimes bigger bubbles passing through such that void fractions increase rapidly. As superficial gas velocity increases, the void fractions fluctuate more violently, and the magnitudes of void fractions increase. Moreover, most big bubbles appear at sub-channel and rod-wall. The averaged void fractions under various test conditions are shown in Fig. 5. At very low superficial fluid velocity, the void fraction of rod-wall is much lower than the others. As the superficial fluid velocity is equal to 0.142 m/s, the void fraction values of sub-channel, rod-gap, and rod-wall are nearly the same.

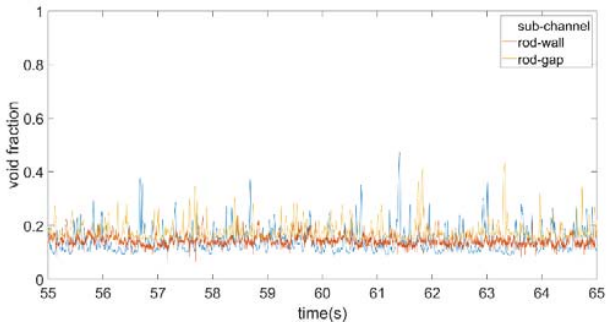

(a) J_f=0.142 m/s, J_g=0.047 m/s

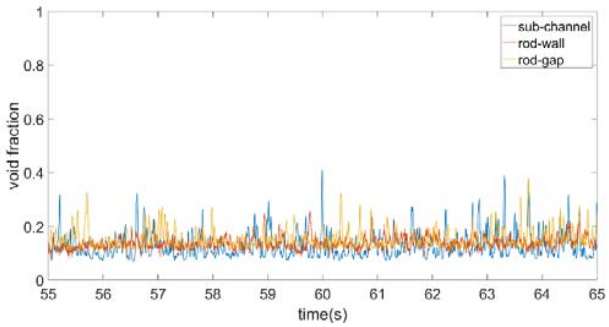

(b) J_f=0.142 m/s, J_g=0.094 m/s

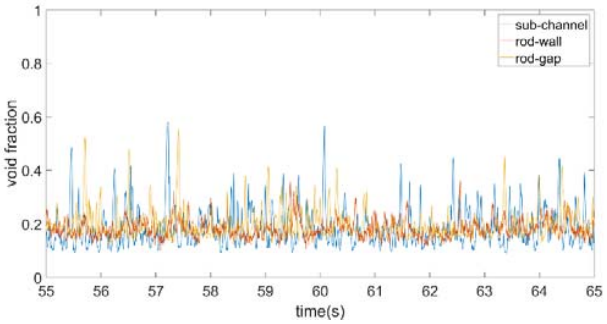

(c) J_f=0.142 m/s, J_g=0.165 m/s

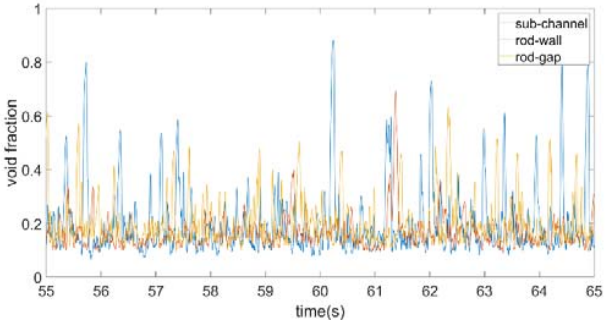

(d) J_f=0.142 m/s, J_g=0.236 m/s

Fig. 4 Void fraction signals under various test conditions

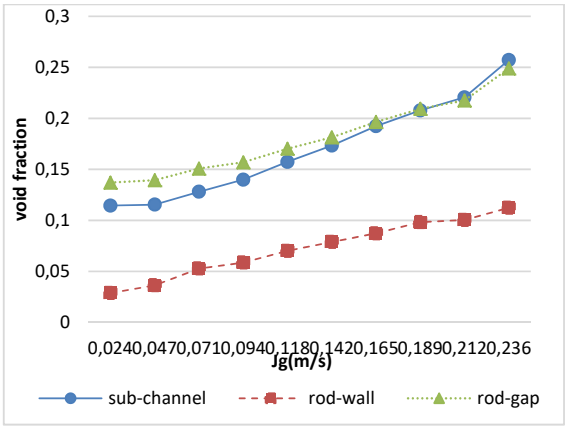

(a) J_f=0.024 m/s

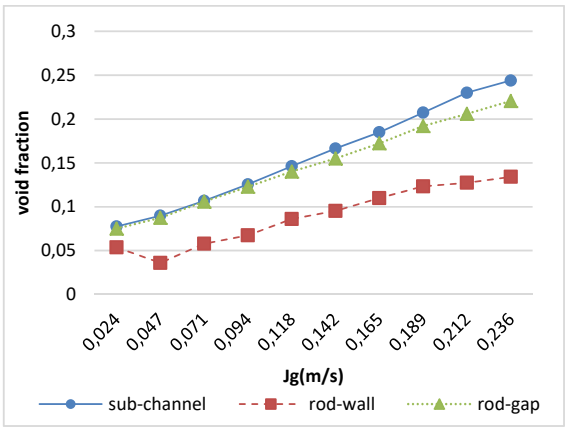

(b) J_f=0.099 m/s

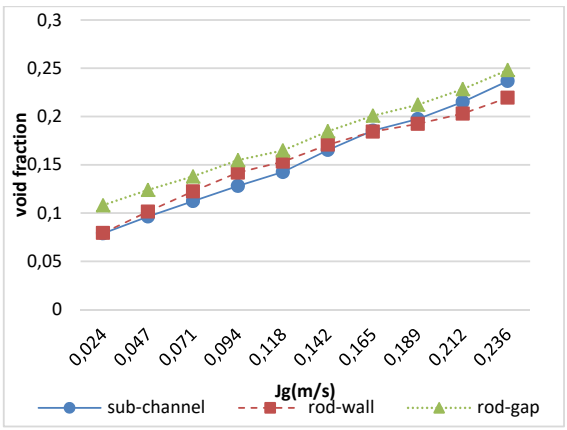

(c) J_f=0.142 m/s

Fig. 5 Averaged void fraction under various test conditions

IV. Conclusion

In this study, experimental tests of air-water two-phase flow in a 3 x 3 rod bundle test section have been carried out. The test flow conditions covered the ranges of $J_f \approx$ 0.024, 0.099 and 0.142 m/s, and $J_g \approx$ 0.024-0.236 m/s. The local void fraction signals can be measured by the conductivity probes at various

local regions such as rod-gap, sub-channel and rod-wall regions. In addition, the photos of two-phase flow mixtures flow in the rod bundle geometry were taken by the high speed camera and used for visual analyses of flow patterns and void distribution. The major conclusions are briefly summarized as follows.

(1) The bubble size and void fraction will be larger as superficial gas velocity increases under constant superficial fluid velocity flow conditions. While superficial gas velocity increases, small bubbles may start to coalesce and gradually become lager bubbles.
(2) All of the averaged local void fractions can increase as the superficial gas velocity increases.
(3) The void fraction of the rod-wall region is much lower than the others when $J_f \leq 0.1$ m/s. As J_f is higher than 0.1 m/s, the bubble distribution can become more uniform throughout the cross section.

ACKNOWLEDGMENT

The authors would like to express their sincere appreciations for the supports from Ministry of Science and Technology (MOST), Atomic Energy Council (AEC) and Taiwan Power Company (TPC) of Taiwan.

REFERENCES

[1] K. Mishima and M. Ishii, "Flow regime transition criteria for upward two-phase flow in vertical tubes," *International Journal of Heat and Mass Transfer*, vol. 27, May 1984, pp. 723-737.
[2] M. Ishii and T. Hibiki, *Thermo-Fluid Dynamics of Two-Phase Flow*. New York, Springer, 2006.
[3] S.W. Chen, Y. Liu, T. Hibiki, M. Ishii, Y. Yoshida, I. Kinoshita, M. Murase, K. Mishima, "One-dimensional drift-flux model for two-phase flow in pool rod bundle systems," *International Journal of Multiphase Flow*, vol.40, pp. 166-177, Apr. 2012.
[4] S.W. Chen, Y. Liu, T. Hibiki, M. Ishii, Y. Yoshida, I. Kinoshita, M. Murase, K. Mishima, "Experimental study of air–water two-phase flow in an 8 × 8 rod bundle under pool condition for one-dimensional drift-flux analysis," *International Journal of Heat and Fluid Flow*, vol.33, pp. 168-181, Feb. 2012.
[5] S.W. Chen, M.S. Lin, F.J. Kuo, M.L. Chai, S.Y. Liu, J.D. Lee, B.S. Pei, "Experimental Investigation and Identification of the Transition Boundary of Churn and Annular Flows using Multi-Range Differential Pressure and Conductivity Signals", *Applied Thermal Engineering*, vol. 114, pp. 1275–1286, Sep. 2016.